Solar Phys (2007) 242: 101–109
DOI 10.1007/s11207-007-0412-6

# Frequency Distributions of Microwave Pulses for the 18 March 2003 Solar Flare

**Zongjun Ning · H. Wu · F. Xu · X. Meng**

Received: 21 January 2007 / Accepted: 8 April 2007 /
Published online: 1 June 2007
© Springer 2007

**Abstract** We analyze the pulses in high-frequency drift radio structures observed by the spectrometer at Purple Mountain Observatory (PMO) over the frequency range of 4.5 – 7.5 GHz during the 18 March 2003 solar flare. A number of individual pulses are determined from the drifting radio structures after the detected gradual component subtraction. The frequency distributions of microwave pulse occurrence as functions of peak flux, duration, bandwidth, and time interval between two adjacent pulses exhibit a power-law behavior, *i.e.* $\mathrm{d}N/\mathrm{d}x \propto x^{-\alpha_x}$. From regression fitting in log-log space, we obtain the power-law indexes, $\alpha_{\mathrm{P}} = 7.38 \pm 0.40$ for the peak flux, $\alpha_{\mathrm{D}} = 5.39 \pm 0.86$ for the duration, and $\alpha_{\mathrm{B}} = 6.35 \pm 0.56$ for the bandwidth. We find that the frequency distribution for the time interval displays a broken power law. The break occurs at about 500 ms, and their indexes are $\alpha_{W1} = 1.56 \pm 0.08$ and $\alpha_{W2} = 3.19 \pm 0.12$, respectively. Our results are consistent with the previous findings of hard X-ray pulses, type III bursts, and decimetric millisecond spikes.

**Keywords** Flares · Radio radiation

## 1. Introduction

Drifting radio structures and their individual bursts (or pulses) have been well studied in the decimetric and microwave range before (*e.g.*, Karlický and Odstrčil, 1994; Karlický, 1998, 2004; Kliem, Karlický, and Benz, 2000; Hudson *et al.*, 2001; Jiřička *et al.*, 2001; Kundu *et al.*, 2001; Khan *et al.*, 2002; Karlický, Fárník, and Mészárosová, 2002; Karlický and Kosugi, 2004; Karlický *et al.*, 2005; Karlický and Bárta, 2007). They were found to be a radio signature of a plasmoid ejection at the beginning of some eruptive solar flares (*e.g.*, Karlický and Odstrčil, 1994; Khan *et al.*, 2002; Karlický, Fárník, and Mészárosová, 2002). The global frequency drift of the structure was explained by a plasmoid propagation upward in the solar corona toward lower plasma densities. Based on MHD numerical simulations, Kliem,

Z. Ning (✉) · H. Wu · F. Xu · X. Meng
Purple Mountain Observatory, Nanjing 210093, People's Republic of China
e-mail: ningzongjun@pmo.ac.cn

Karlický, and Benz (2000) suggested that each pulse in the drifting structures is generated by a beam of superthermal electrons accelerated by the electric field in the reconnection region.

We presented the observational characteristics of high-frequency drift radio structures observed by the spectrometer at Purple Mountain Observatory (PMO) over the frequency range of 4.5 – 7.5 GHz during the 18 March 2003 solar flare in our previous paper (Ning *et al.*, 2007; henceforth Paper I) in detail. These radio structures are observed before the soft X-ray maximum, almost at the peak of hard X rays at 25 – 50 keV. The microwave pulses of drifting structures show an average duration of 36.3 ms. In this paper, we will study the frequency distributions of pulse occurrence as functions of the peak flux, the duration, the bandwidths and the time interval between adjacent pulses.

Frequency distributions have been calculated for various types of flare-associated activities, such as radio bursts, soft X rays, hard X rays, interplanetary type III bursts, interplanetary particle events, and CMEs (*e.g.*, Dennis, 1985; Lu and Hamilton, 1991; Lu *et al.*, 1993; Crosby, Aschwanden, and Dennis, 1993; Aschwanden, Schwartz, and Alt, 1995; Boffetta *et al.*, 1999; Wheatland and Sturrock, 1996; Wheatland, Sturrock, and McTiernan, 1998; Wheatland and Litvinenko, 2002; Wheatland, 2000, 2003; Craig, 2001; Paczuski, Boettcher, and Baiesi, 2005; Aschwanden, Dennis, and Benz, 1998; Aschwanden and Parnell, 2002; Veronig *et al.*, 2002; Nita, Gary, and Lee, 2004; Qiu *et al.*, 2004; Baiesi, Paczuski, and Stella, 2006; de Arcangelis *et al.*, 2006; Su, Gan, and Li, 2006). It has been shown that above a certain threshold (often attributed to the sensitivity of the observations) most of these frequency distributions can be represented by power laws of the form $\mathrm{d}N \propto x^{-\alpha_x}\,\mathrm{d}x$, where $\mathrm{d}N$ denotes the number of events recorded with the parameter $x$ of interest in the interval $[x, x + \mathrm{d}x]$ and $\alpha_x$ is a constant, which can be determined from a fit to the data.

## 2. Observations and Data Analysis

The data we use here are collected by the radio spectrometer at PMO, China. It has 300 frequency channels, each with a 10-MHz bandwidth and a time resolution of 10 ms. Its daily working time is between 1:00 and 9:00 UT. This spectrometer has recorded many events during the 23rd solar cycle since 1998 (*e.g.*, Xu and Wu, 2004; Wu, Xu, and Huang, 2004; Ning *et al.*, 2003, 2005). A good description of this instrument can be found in the paper by Xu *et al.* (2003).

On 18 March 2003, the GOES satellite observed a soft X-ray flare that started at 05:51 UT, reached its maximum at 06:00 UT, and ended at 06:02 UT. This class M2.5 event was localized at the active region NOAA AR 10314. According to Hα observations the 1N flare was detected from 05:54 UT (start) to 06:00 UT (maximum) to 06:21 UT (end) at S15W46. Figure 1 shows the soft X-ray and microwave emissions of this event. An impulsive peak is simultaneously observed by the PMO spectrometer and the Nobeyama Radio Polarimeter (NoRP; Nakajima *et al.*, 1985) between 05:59 and 06:00 UT, which is the same time as the maximum of soft X rays. The dynamic spectra of radio bursts display four groups of drifting structures (bottom panel). It is clear that these structures are drifting out of the high-frequency limit of 7.5 GHz of the PMO spectrometer. NoRP observations suggest that the drifting structures extend, at least, to a frequency of 9.4 GHz. The EUV, hard X-ray, and microwave radio images were presented in Paper I.

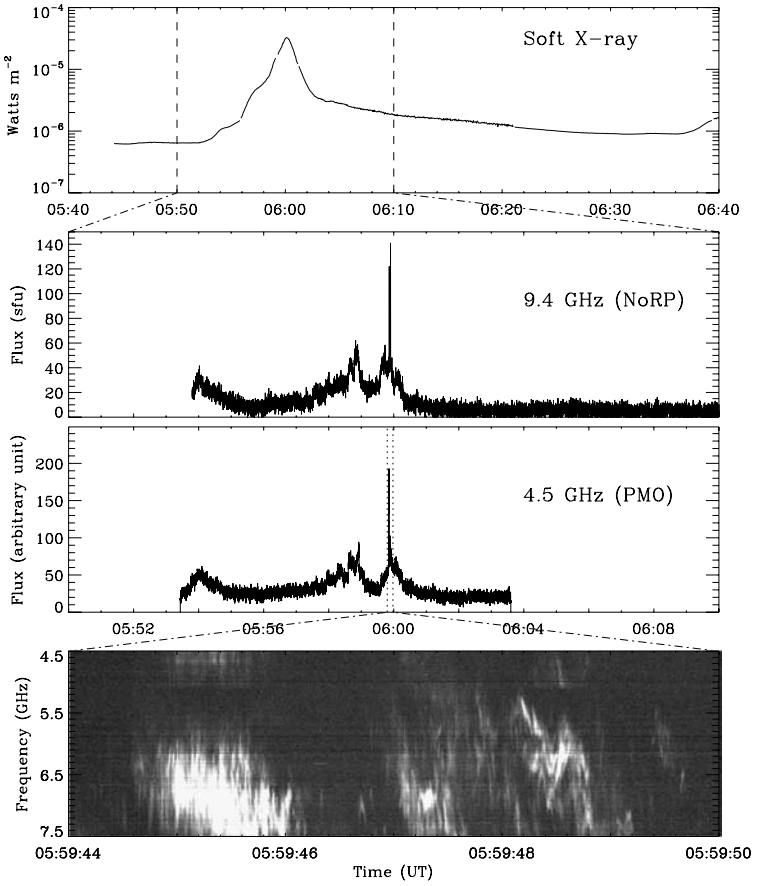


**Figure 1** An overview of solar flare detected by soft X-ray and microwave emissions on 18 March 2003. Top panel: Flux of GOES soft X rays at 1 – 8 Å. Second panel: Microwave bursts observed by NoRP at 9.4 GHz. Third panel: Microwave bursts observed by the PMO spectrometer at 4.5 GHz. Bottom panel: Dynamic spectra of the positively drifting structures observed by the PMO spectrometer. (This figure has been previously published in Paper I.)

## 2.1. Microwave Pulses

To investigate pulses of drifting structures, we first have to decompose the drifting structures from the flare gradual component. However, to properly measure the gradual component from the observations is very difficult, and it can never be done perfectly. In our previous Paper I, the gradual component is determined as a constant background emission. In fact, the gradual component of microwave emission should be a function of time. Based on the method by Aschwanden, Dennis, and Benz (1998) for determining the pulse in hard X-ray emission, the lower envelope of the bursts is identified as the gradual component. Drifting structures are determined by the microwave bursts after subtraction of the detected gradual component. Figure 2 shows the microwave bursts, the detected gradual component, and the drifting structures at 6.8 GHz in a short time interval between 05:59:45.300 and 05:59:45.600 UT.

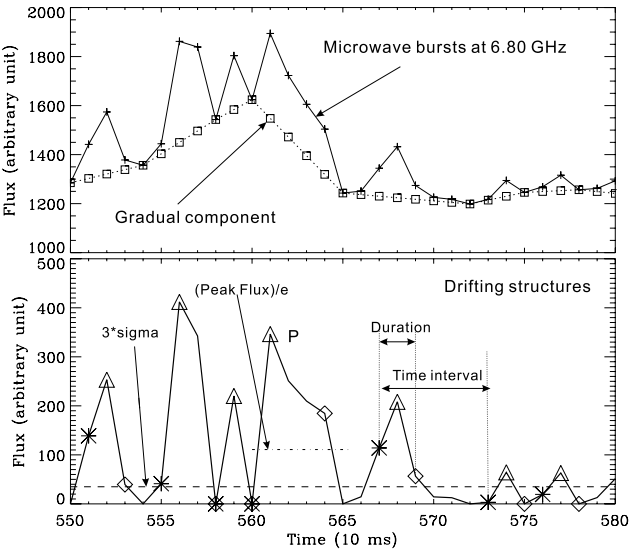


**Figure 2** Top panel: Microwave bursts (pluses) and the detected gradual component (squares) at 6.8 GHz between 05:59:45.300 and 05:59:45.600 UT. Bottom panel: Interpretation of pulse duration and time interval in this paper. The points marked with stars before the peaks (triangles) are identified as the start times of pulses; the diamonds after the peaks are the end times. The dot-dashed line represents the level of the exponent of peak flux at $X = 561$ (see details in text). The number e is the base of the natural logarithm.

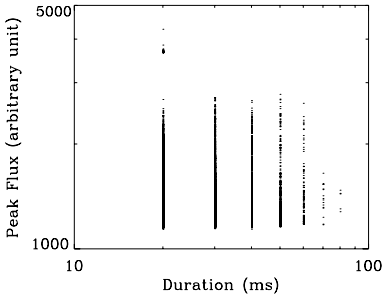


**Figure 3** Dependence of pulse duration on peak flux.

Then we have to determine the profile of each pulse. First, we have to determine the flux peak of each pulse. A value of $3\sigma$ is used as the criteria of pulse peaks, where sigma is computed from the quiet Sun emission at each frequency channel. If a point represents a local maximum of the flux above the $3\sigma$ level, it is identified as the flux peak of a pulse profile. Thus seven pulse peaks are determined at 6.8 GHz during 05:59:45.300 to 05:59:45.600 UT, as shown in Figure 2 marked by the triangle. Then, we have to determine the start and end times of each pulse. For a given pulse profile, if there is only one point following its peak before the flux rises again, this point is thought to be the end time of this pulse. Otherwise, if there are two or more points following this peak before the flux starts increasing again, we choose the end of a pulse as the point whose flux is close to the value of exponent of peak flux. The start time of the pulse is determined by the same method. Figure 2 (bottom panel) shows the details of how to determine the start and end times of pulses. The start and end times are marked by stars and diamonds, respectively. For example, the start time of the pulse with peak P ($X = 561$) is the preceding point marked with a star ($X = 560$), which is the only point before peak P. However, the end time of this pulse is the point at $X = 564$, which is chosen from the following four points ($X = 562$, 563, 564, and 565) whose flux values are monotonically decreasing with time. The point at $X = 564$ has a flux close to the value of the exponent of peak flux at P (where the dot-dashed line represents the level of

exponent of peak flux at P). In this case, the start and end times of the pulse are related to the peak flux of the pulse. It is possible that the end time of the preceding pulse is the same as the start of the following one. Finally, the duration of an individual pulse is calculated by subtracting the end and start times, and the time interval is between the start times of the preceding and following pulses. Figure 2 (bottom panel) explains their definition in this paper. Figure 3 plots the dependence of pulse duration versus peak flux.

## 2.2. Pulse Bandwidth

To investigate the frequency bandwidth of each individual pulse, we assume that the microwave burst spectrum is a pulse spectrum superimposed on the background spectrum. However, to properly measure the background spectrum from the observations is very difficult. As in the method to determine the gradual component before, Figure 4 shows that the lower envelope of the burst spectrum is identified as the background spectrum. The pulse spectrum is the microwave burst spectrum after the detected background spectrum subtraction. If a point represents a local maximum of the flux above the $3\sigma'$ level, it is identified as the peak of a pulse spectrum. Here $\sigma'$ is the standard deviation of quiet Sun emission at a limited frequency range, *i.e.*, between 4.5 and 5.5 GHz in Figure 4. There are seven pulse spectral profiles to be determined. For a given pulse spectrum, if there is only one point at higher frequency whose flux is smaller than peak value, this point is thought to be the upper

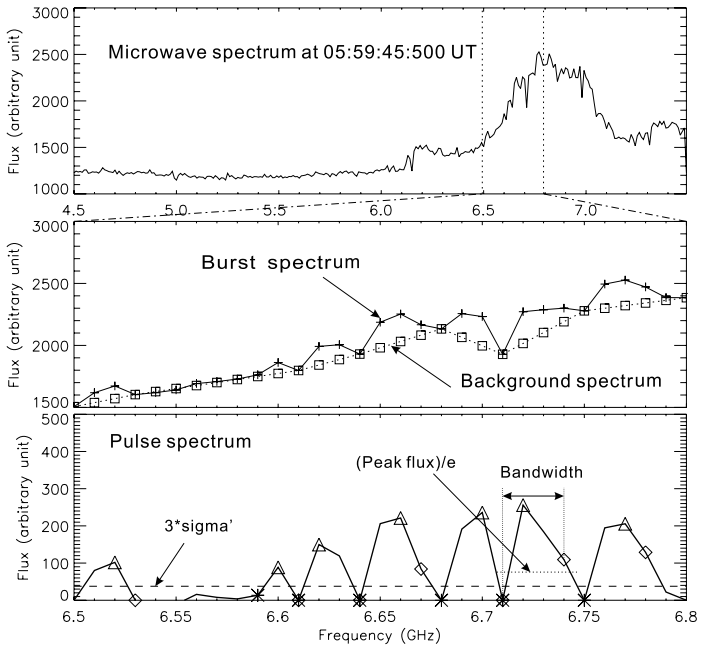


**Figure 4** Top panel: Microwave spectrum at the frequency range between 4.5 and 7.5 GHz at 05:59:45:500 UT. Second panel: Microwave spectrum (pluses) and the detected background spectrum (squares) at the frequency band between 6.5 and 6.8 GHz. Bottom panel: Determination of each individual pulse bandwidth in this paper. The points marked with stars after the peaks (triangles) are identified as the low-frequency limits of pulses; the diamonds before the peaks are the high-frequency limits. The dot-dashed line represents the level of the exponent of the peak flux at 6.72 GHz (see details in text). The number e is the base of the natural logarithm.

limit of this pulse spectrum. Otherwise, if there are two or more points at higher frequencies whose fluxes are monotonically decreasing with increasing frequency, we choose the upper limit of a pulse spectrum as the point whose flux is close to the value of the exponent of peak flux. The lower limit of the pulse spectrum is determined by the same method. The pulse bandwidth is thought to be the frequency interval between the upper and lower limits. Figure 4 (bottom panel) shows the details of how to determine the pulse bandwidth. The lower and upper limits are marked by stars and diamonds, respectively. For example, the lower limit of pulse spectrum with a peak at 6.72 GHz is the preceding point marked with a star at a frequency of 6.71 GHz, which is the only point below 6.72 GHz before the flux starts increasing with decreasing frequency. However, the upper limit of the pulse spectrum is 6.74 GHz, which is chosen from the three points ($F = 6.73$, 6.74, and 6.75 GHz) whose flux values are monotonically decreasing with increasing frequency. The point at 6.74 GHz has a flux close to the value of the exponent of the peak flux at 6.72 GHz (dot-dashed line). It is possible that the upper limit of the preceding pulse is the same as the lower limit of the following one.

## 3. Results

Using the method in Section 2, we determine the profile and spectrum of each individual pulse are for 300 frequency channels between 05:59:44 and 05:59:50 UT. Thus we get the peak flux, duration, and bandwidth of each pulse and time interval between adjacent pulses. Our results show that the peak flux of microwave pulses is independent of the duration, as shown in Figure 3. Figure 5 gives their number histograms, which are similar to the distribution of peak time separations found by Karlický, Fárník, and Mészárosová (2002).

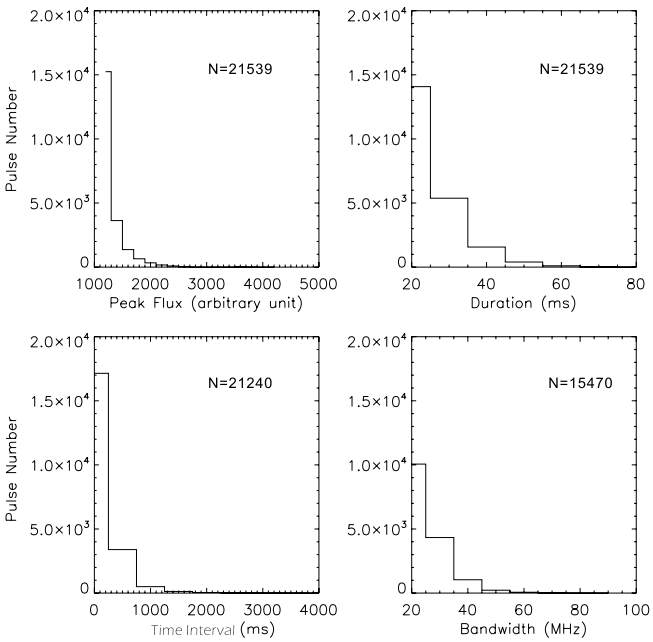


**Figure 5** Histograms of pulse peak flux, duration, time interval, and bandwidth.

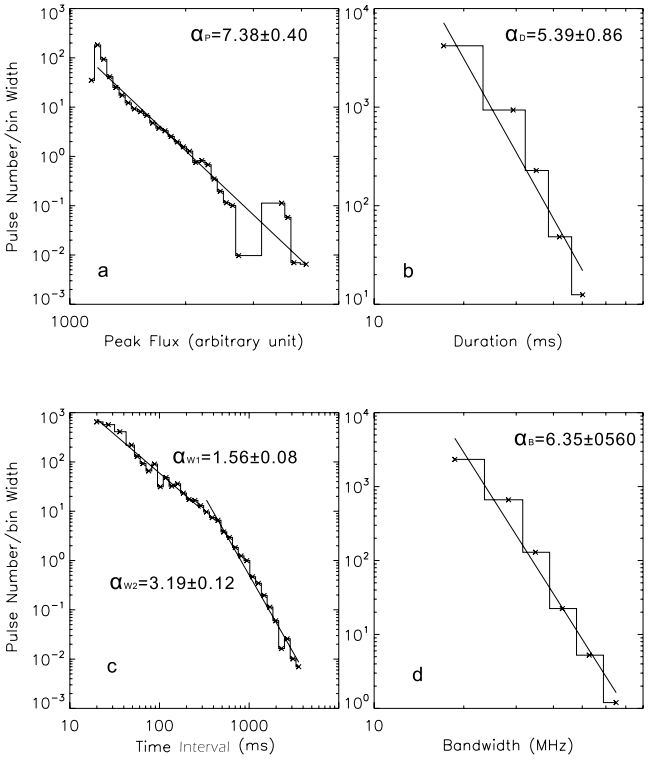


**Figure 6** Frequency distributions as functions of the peak flux, duration, time interval, and bandwidth.

The number histogram of pulse duration is similar to the result in Paper I. But many more pulses are detected than before owing to the smaller criteria value to determine the pulse.

Figure 6 shows the frequency distributions as functions of the peak flux, the duration, the time interval, and the bandwidth. They exhibit a power-law behavior as $\mathrm{d}N/\mathrm{d}x \propto x^{-\alpha_x}$ (where $x$ represents the peak flux or duration or time interval or bandwidth). This is consistent with the previous findings for hard X-ray pulses, type III bursts, and decimetric millisecond spikes (*e.g.*, Aschwanden, Dennis, and Benz, 1998). From the slopes of the distributions in log-log space we obtain the power-law indexes $\alpha_{\mathrm{P}} = 7.38 \pm 0.40$ for peak flux, $\alpha_{\mathrm{D}} = 5.39 \pm 0.86$ for duration, and $\alpha_{\mathrm{B}} = 6.35 \pm 0.56$ for bandwidth. The frequency distribution of time interval displays a broken power law. The break occurs at about 500 ms, and their indexes are $\alpha_{W1} = 1.56 \pm 0.08$ and $\alpha_{W2} = 3.19 \pm 0.12$.

The fact that the frequency distribution of the time interval exhibits a broken power-law behavior is related to the observational characteristics of this event. As noted earlier, four groups of drifting structures are observed. The pulses with a big time interval could be at the time between the end of the preceding group and the beginning of the following one, while most of the pulses within each group are separated by a short time interval. Thus, their frequency distribution shows a break at 500 ms, which is the same as the average time interval between the adjacent groups.

## 4. Discussion

Sturrock *et al.* (1984) pointed out that a flare is a consequence of many small reconnection events (or elementary bursts) and that sub-bursts (pulses) are an observational signature of the elementary bursts in solar flares. Later, Parker (1989) modified this concept by adding the spontaneous current sheets that arise throughout the field subject to any continuous random displacement of the footpoints at the photosphere. Based on previous observations, Karlický (2004) suggested the fragmentation process to explain the decimetric or microwave drift radio structures. In such a scenario the microwave pulses can be considered as the radio emissions from the turbulent reconnection region plasma. The duration and bandwidth of the detected pulses might be related to the time and spatial scales of turbulence, whereas the time interval between two adjacent pulses might be determined by the tearing instability process (Karlický, 2004).

A general way to derive information about elementary processes in solar flares is to study the pulse in hard X-ray and microwave emissions. Aschwanden, Dennis, and Benz (1998) found that the frequency distributions of hard X-ray pulses, type III bursts, and decimetric millisecond spikes follow a power-law behavior. The microwave pulses display a shorter duration than that of the decimetric radio structures. For the first time, we find that the frequency distributions of microwave pulse occurrence as functions of peak flux, duration, time interval, and bandwidth exhibit a power-law behavior. From the regression fitting, we get the power-law index $\alpha_P = 7.38 \pm 0.40$ for the peak flux of microwave pulses, which is bigger than that for hard X-ray pulses ($1.46 \pm 0.34$) or type III bursts ($1.45 \pm 0.31$) or decimetric pulsations ($1.33 \pm 0.11$) or that for decimetric millisecond spikes ($2.99 \pm 0.63$) (Aschwanden, Dennis, and Benz, 1998). This suggests many more pulses are observed with small flux during the 18 March 2003 flare. It is possible that the power-law index would be related to frequency.

**Acknowledgements** We would like to thank the referee for the constructive comments to improve the manuscript. This work is supported by Grant Nos. Y0607221222, 10333030, 10603014, and the 973 Program (2006CB806302).

## References

Aschwanden, M.J., Parnell, C.E.: 2002, *Astrophys. J.* **572**, 1048.
Aschwanden, M.J., Dennis, B.R., Benz, A.O.: 1998, *Astrophys. J.* **497**, 972.
Aschwanden, M.J., Schwartz, R.A., Alt, D.M.: 1995, *Astrophys. J.* **447**, 923.
Baiesi, M., Paczuski, M., Stella, A.L.: 2006, *Phys. Rev. Lett.* **96**, 051103.
Boffetta, G., Carbone, V., Giuliani, P., Veltri, P., Vulpiani, A.: 1999, *Phys. Rev. Lett.* **83**, 4662.
Craig, I.J.D.: 2001, *Solar Phys.* **202**, 109.
Crosby, N., Aschwanden, M., Dennis, B.: 1993, *Adv. Space Res.* **13**, 179.
de Arcangelis, L., Godano, C., Lippiello, E., Nicodemi, M.: 2006, *Phys. Rev. Lett.* **96**, 051102.
Dennis, B.R.: 1985, *Solar Phys.* **100**, 465.
Hudson, H.S., Kosugi, T., Nitta, N.V., Shimojo, M.: 2001, *Astrophys. J.* **561**, L211.
Jiřička, K., Karlický, M., Mészárosová, H., Snížek, V.: 2001, *Astron. Astrophys.* **375**, 243.
Karlický, M.: 1998, *Astron. Astrophys.* **338**, 1084.
Karlický, M.: 2004, *Astron. Astrophys.* **417**, 325.
Karlický, M., Bárta, M.: 2007, *Astron. Astrophys.* **464**, 735.
Karlický, M., Kosugi, T.: 2004, *Astron. Astrophys.* **419**, 1159.
Karlický, M., Odstrčil, D.: 1994, *Solar Phys.* **155**, 171.
Karlický, M., Bárta, M., Mészárosová, H., Zlobec, P.: 2005, *Astron. Astrophys.* **432**, 705.
Karlický, M., Fárník, F., Mészárosová, H.: 2002, *Astron. Astrophys.* **395**, 677.
Khan, J.I., Vilmer, N., Saint-Hilaire, P., Benz, A.O.: 2002, *Astron. Astrophys.* **388**, 363.

Kliem, B., Karlický, M., Benz, A.O.: 2000, *Astron. Astrophys.* **360**, 715.
Kundu, M.R., White, S.M., Shibasaki, K., Sakurai, T., Grechnev, V.V.: 2001, *Astrophys. J.* **547**, 1090.
Lu, E.T., Hamilton, R.J.: 1991, *Astrophys. J.* **380**, L89.
Lu, E.T., Hamilton, R.J., McTiernan, J.M., Bromund, K.R.: 1993, *Astrophys. J.* **412**, 841.
Nakajima, H., Sekiguchi, H., Sawa, M., Kai, K., Kawashima, S.: 1985, *Publ. Astron. Soc. Japan* **37**, 163.
Ning, Z.-J., Liu, Y.-Y., Fu, Q.-J., Xu, F.-Y.: 2003, *Chin. J. Astron. Astrophys.* **3**, 381.
Ning, Z., Ding, M.D., Wu, H.A., Xu, F.Y., Meng, X.: 2005, *Astron. Astrophys.* **437**, 691.
Ning, Z., Wu, H.A., Xu, F.Y., Meng, X.: 2007, *Solar Phys.* **241**, 77.
Nita, G.M., Gary, D.E., Lee, J.: 2004, *Astrophys. J.* **605**, 528.
Parker, E.N.: 1989, *Solar Phys.* **121**, 271.
Paczuski, M., Boettcher, S., Baiesi, M.: 2005, *Phys. Rev. Lett.* **95**, 181102.
Qiu, J., Liu, C., Gary, D.E., Nita, G.M., Wang, H.: 2004, *Astrophys. J.* **612**, 530.
Sturrock, P.A., Kaufman, P., Moore, R.L., Smith, D.F.: 1984, *Solar Phys.* **94**, 341.
Su, Y., Gan, W.Q., Li, Y.P.: 2006, *Solar Phys.* **238**, 61.
Veronig, A., Temmer, M., Hanslmeier, A., Otruba, W., Messerotti, M.: 2002, *Astron. Astrophys.* **382**, 1070.
Wheatland, M.S.: 2000, *Astrophys. J.* **536**, L109.
Wheatland, M.S.: 2003, *Solar Phys.* **214**, 361.
Wheatland, M.S., Litvinenko, Y.E.: 2002, *Solar Phys.* **211**, 255.
Wheatland, M.S., Sturrock, P.A.: 1996, *Astrophys. J.* **471**, 1044.
Wheatland, M.S., Sturrock, P.A., McTiernan, J.M.: 1998, *Astrophys. J.* **509**, 448.
Wu, H., Xu, F., Huang, G.-L.: 2004, In: Dupree, A.K., Benz, A.O. (eds.) *Stars and Suns: Activity, Evolution and Planets*, *Proc. IAU Symp.* **219**, 717.
Xu, F.-Y., Xu, Z.-C., Huang, G.-I., Yao, Q.-J., Meng, X., Wu, H.-A.: 2003, *Solar Phys.* **216**, 273.
Xu, F.Y., Wu, H.A.: 2004, *Astron. Astrophys.* **425**, 281.